

Nuclear Factor I Represses the Notch Effector *HEY1* in Glioblastoma¹



Miranda Brun², Saket Jain², Elizabeth A. Monckton and Roseline Godbout

Department of Oncology, Faculty of Medicine and Dentistry, University of Alberta, Edmonton, Alberta, Canada, T6G 1Z2

Abstract

Glioblastomas (GBMs) are highly aggressive brain tumors with a dismal prognosis. Nuclear factor I (NFI) is a family of transcription factors that controls glial cell differentiation in the developing central nervous system. NFIs have previously been shown to regulate the expression of astrocyte markers such as glial fibrillary acidic protein (*GFAP*) in both normal brain and GBM cells. We used chromatin immunoprecipitation (ChIP)–on-chip to identify additional NFI targets in GBM cells. Analysis of our ChIP data revealed ~400 putative NFI target genes including an effector of the Notch signaling pathway, *HEY1*, implicated in the maintenance of neural stem cells. All four NFIs (NFIA, NFIB, NFIC, and NFIX) bind to NFI recognition sites located within 1 kb upstream of the *HEY1* transcription site. We further showed that NFI negatively regulates *HEY1* expression, with knockdown of all four NFIs in GBM cells resulting in increased *HEY1* RNA levels. *HEY1* knockdown in GBM cells decreased cell proliferation, increased cell migration, and decreased neurosphere formation. Finally, we found a general correlation between elevated levels of *HEY1* and expression of the brain neural stem/progenitor cell marker *B-FABP* in GBM cell lines. Knockdown of *HEY1* resulted in an increase in the RNA levels of the *GFAP* astrocyte differentiation marker. Overall, our data indicate that *HEY1* is negatively regulated by NFI family members and is associated with increased proliferation, decreased migration, and increased stem cell properties in GBM cells.

Neoplasia (2018) 20, 1023–1037

Introduction

Glioblastomas (GBMs) (or grade IV astrocytomas) are the most common brain tumors in adults [1,2]. Despite aggressive treatment involving surgical resection, radiotherapy, and adjuvant chemotherapy with temozolomide, the median survival for GBM patients is approximately 15 months [3–5]. These tumors are highly infiltrative, resulting in high rates of recurrence and treatment failure [6].

The Nuclear Factor I (NFI) family of transcription factors regulates the expression of the brain fatty acid-binding protein (*B-FABP* or *FABP7*) and glial fibrillary acidic protein (*GFAP*) genes in GBM [7]. The four members of the NFI family (NFIA, B, C, and X) bind to the consensus NFI recognition element 5'-TTGGCA(N₅)GCCAA-3' as homodimers or heterodimers [8–10]. The N-terminal DNA binding and dimerization domain of all four NFI family members is highly conserved; however, the C-terminal domain is more divergent, resulting in variation in transactivation potential [11]. NFIs can both activate or repress transcription, with regulation of transcription being dependent on both promoter context and type of cell or tissue in which the NFIs are expressed [12].

NFI recognition sites are enriched in many brain-specific promoters [13], and NFIs are important regulators of gliogenesis

and astrocyte differentiation in the developing central nervous system [14–16]. In particular, NFIA and NFIB are necessary for the onset of gliogenesis downstream of Notch signaling [15,17]. Following glial fate specification, these two NFIs along with NFIX further promote

Abbreviations: APCDD1, adenomatous polyposis coli downregulated 1; AP2, activating protein 2; bHLH, basic helix-loop-helix; B-FABP, brain fatty acid-binding protein; CoRE, composite response element; EZH2, enhancer of zest homolog 2; GBM, glioblastoma; GO, gene ontology; GFAP, glial fibrillary acidic protein; HES1, hairy and enhancer of split-1; HEY1, Hes related family BHLH transcription factor with YRPW motif 1; MMD2, monocyte to macrophage differentiation associated 2; MMTV, mouse mammary tumor virus; NEFL, neurofilament light; NFI, nuclear factor I; PAX-6, paired box protein-6; PET, polyethylene terephthalate; SPARCL1, SPARC like protein 1; WAP, whey acidic protein gene. Address all correspondence to: Roseline Godbout, Department of Oncology, Cross Cancer Institute, 11560 University Avenue, Edmonton, Alberta T6G 1Z2, Canada. E-mail: rgodbout@ualberta.ca

¹ Declarations of Interest: The authors declare that they have no conflicts of interest.

² These authors contributed equally to the manuscript.

Received 16 April 2018; Revised 17 August 2018; Accepted 20 August 2018

© 2018 The Authors. Published by Elsevier Inc. on behalf of Neoplasia Press, Inc. This is an open access article under the CC BY-NC-ND license (<http://creativecommons.org/licenses/by-nc-nd/4.0/>). 1476-5586

<https://doi.org/10.1016/j.neo.2018.08.007>

astrocyte differentiation [14,16,18–20]. *Nfia*^{-/-}, *Nfib*^{-/-}, and *Nfix*^{-/-} mice all display delayed neuronal and glial cell differentiation in the brain [21–27].

Reduced *NFIA* mRNA levels are associated with high-grade astrocytomas, with 91%, 77%, 48%, and 37% of cells expressing *NFIA* in grades I, II, III, and IV astrocytomas, respectively [28,29]. *NFIA* is enriched in astrocytomas compared to other tumors, with fewer than 5% of cells expressing *NFIA* in oligodendrogliomas [28]. Furthermore, ectopic expression of *NFIA* in an oligodendroglioma model promotes conversion to an astrocytoma-like phenotype [19]. Low *NFIB* mRNA levels are also associated with high-grade astrocytomas, with elevated levels of *NFIB* RNA correlating with better overall and recurrence-free survival in GBM [30]. *NFIB* overexpression induces cell differentiation and inhibits GBM tumor growth [30].

To gain insight into the role of NFI in GBM, we carried out chromatin immunoprecipitation (ChIP)–on-chip using a pan-specific NFI antibody to immunoprecipitate NFIs bound to their target genes in U251 GBM cells. A total of 403 NFI target genes were identified, including *HEY1*, a Notch effector gene. Notch signaling has previously been implicated in regulation of tumor progression in GBM [31–33]. *HEY1* is a member of the Hairy/Enhancer of split (E/spl) family of basic helix-loop-helix transcription factors and is important for maintenance of neural precursor cells downstream of Notch [34]. *HEY1* expression increases with increasing astrocytoma tumor grade and correlates with decreased overall survival and disease-free survival [35]. Here, we show that NFI binds to three NFI recognition elements in the *HEY1* promoter and negatively regulates *HEY1* in GBM cells. Depletion of *HEY1* in adherent and neurosphere GBM cultures results in decreased cell proliferation, increased migration, and decreased neurosphere formation. These results suggest a fine balance between levels of NFI transcription factors and the Notch effector *HEY1* in GBM, thereby allowing these tumors to express some astrocytic properties while retaining neural stem cell characteristics.

Materials and Methods

Cell Lines, Constructs, siRNAs, and Transfections

The established human GBM cell lines used in this study have been previously described [36,37]. Cells were cultured in Dulbecco's modification of Eagle's minimum essential medium (DMEM) supplemented with 10% fetal calf serum, penicillin (50 U/ml), and streptomycin (50 µg/ml). The primary GBM cultures (A4-004, A4-007, ED512) were prepared by enzymatic dissociation of GBM biopsies obtained with patient consent prior to surgery. A4-004 and A4-007 adherent lines were generated by culturing cells directly in DMEM supplemented with 10% fetal calf serum. GBM tumor neurosphere cultures were generated by plating cells directly in DMEM/F12, supplemented with B27, epidermal growth factor, and fibroblast growth factor. All procedures involving tumor biopsies were approved by the Health Research Ethics Board of Alberta Cancer Committee Protocol #HREBA.CC-14-0070.

The pCH-NFI expression vectors pCH, pCH-NFIA, pCH-NFIB, pCH-NFIC, and pCH-NFIX were obtained from Dr. R. Gronostajski (State University of New York at Buffalo). The luciferase reporter gene construct was prepared by inserting the 5' *HEY1* flanking DNA from –913 bp to +15 bp into the pGL3-Basic vector (Promega). Stealth siRNAs (Life Technologies) were used to

knockdown *NFIA*, *NFIB*, *NFIC*, *NFIX*, and *HEY1*: NM_005595_stealth_919 targeting 5'-GAAAGUUCUUAUAUCUACAG-CAUGA-3' (*NFIA*); NM_005596_stealth_1020 targeting 5'-AAGCCACAAUGA-UCCUGCCAAGAAU-3' (*NFIB*); NM_005597_stealth_1045 targeting 5'-CAGAGAU-GGACAA-GUCACCAUUCAA-3' (*NFIC*); NM_002501_stealth_752 targeting 5'-GAGAGUAUCACAGACUCCUGUUGCA-3' (*NFIX*); NM_012258.3_stealth_284 targeting 5'-UAGAGCCGAACU-CAAGUUUCCAUUC-3' (*HEY1* siRNA 1); and NM_012258.3_stealth_652 targeting 5'-UUGAGAUGCAGAAAC-CAGUCGAACUC-3' (*HEY1* siRNA 2). Scrambled siRNAs (cat. nos. 12935-200 and 12935-300) were used as negative controls. The Stealth siRNAs selected for NFI knockdown have been previously characterized [36].

U251 GBM cells were transfected with plasmid DNA constructs using polyethylenimine (Polysciences Inc.). For knockdown experiments, cells were transfected with 10 nM siRNAs using RNAiMAX-Lipofectamine (Life Technologies). For co-transfection experiments, cells were transfected first with siRNA followed by plasmid transfection 24 hours later. Cells were harvested 60 hours after the last transfection. For 2× transfections with siRNAs, cells were transfected, grown to confluency, replated at 1/7 dilution, and transfected again.

ChIP-on-chip

ChIP to isolate NFI-bound DNA was carried out following Agilent's mammalian ChIP-on-chip protocol version 10.0. Briefly, 8×10^8 U251 GBM cells were cross-linked with 1% formaldehyde for 12 minutes at room temperature, followed by addition of glycine to 0.125 M to terminate the cross-linking reaction. After cell lysis, nuclei were sonicated 30 × 30 seconds at 30% output (model 300VT, Ultrasonic Homogenizer, BioLogics, Inc.), and Triton X-100 was added to a final concentration of 1%. Cellular debris was removed by centrifugation, and 50 µl of the lysate was frozen at –20°C for input DNA (nonenriched control). The remaining lysate was precleared with Protein-A Sepharose beads (GE Healthcare). The precleared lysate was incubated with 3 µg anti-NFI antibody (N-20 Santa Cruz Biotechnology) and incubated at 4°C for 16 hours. Protein-A Sepharose beads were added and incubated for 2 hours at 4°C. Beads were washed 7× in wash buffer (50 mM Hepes-KOH, 500 mM LiCl, 1 mM EDTA, 1% Nonidet-P40, 0.7% sodium deoxycholate) and 1× in TE with 50 mM NaCl at 4°C. Protein-DNA complexes were eluted in elution buffer (50 mM Tris-HCl pH 8.0, 10 mM EDTA, 1% SDS) at 65°C for 15 minutes.

Linkers (5'-GCGGTGACCCGGGAGATCTGAATTC-3', and 5'-GAATTCAGATC-3') were prepared by annealing at 70°C for 1 minute and cooling slowly to 4°C. Input and ChIP DNAs were amplified by LM-PCR. PCRs containing input or ChIP DNAs, 1× Thermopol buffer (NEB), 250 µM dNTPs, 1 µM LM-PCR primer 5'-GCGGTGACCCGGGAGATCTGAATTC-3', and 0.25 U Taq polymerase were carried out as follows: 55°C/4 min, 72°C/3 min, 95°C/2 min, (95°C/30 s, 60°C/30 s, 72°C/1 min) × 15, 72°C/5 min. One hundredth of the resulting PCR products was used in a second round of PCR amplification as described above for 25 cycles. The PCR products were precipitated with ethanol, resuspended in sterile H₂O, and diluted to 100 ng/µl.

Input and ChIP DNAs were fluorescently labeled with Agilent Genomic DNA Labeling Kit PLUS (Agilent Technologies). For each reaction, 2 µg input or ChIP DNA was incubated with 5 µl random

primers, 1× buffer, 1× dNTPs, 3 μl 1.0 mM Cyanine 3-dUTP (Cy3) (input DNA) or 3 μl 1.0 mM Cyanine 5-dUTP (Cy5) (ChIP DNA), and 1 μl Exo-Klenow DNA polymerase fragment in a final volume of 50 μl and incubated at 37°C for 2 hours followed by 10-minute incubation at 65°C to inactivate the enzyme. For hybridization, 5 μg Cy3-labeled DNA, 5 μg Cy5-labeled DNA, 50 μg Human Cot1, 1× Agilent blocking agent, and 1× Agilent hybridization buffer per slide were heated for 3 minutes at 95°C followed by incubation at 37°C for 30 minutes and then applied to the Agilent Human Promoter 1 ChIP-on-chip 244K 014706 and 014797 microarray sets (Agilent Technologies) (two independent experiments). Slides were hybridized with shaking (20 RPM) in a hybridization oven at 65°C for 40 hours. The slides were then washed 1× with Oligo aCGH/ChIP-on-chip wash buffer (Agilent Technologies) at room temperature and 1× with Oligo aCGH/ChIP-on-chip wash buffer at 31°C. Slides were scanned on a GenePix 4000B scanner, and data were extracted using Agilent Feature Extraction Software (Agilent Technologies). Data were analyzed using Agilent Genomic Workbench (Agilent Technologies).

ChIP-PCR

ChIP-PCR analysis was carried out as previously described [38]. Briefly, U251 cells cross-linked with 1% formaldehyde were resuspended in lysis buffer and sonicated to shear the DNA. Pre-cleared lysates were incubated with either 2 μg IgG or 2 μg anti-NFI antibody (N-20 Santa Cruz Biotechnology), followed by incubation with Protein A-Sepharose beads. Protein-DNA complexes were eluted, and the DNA was amplified using primers flanking putative NFI binding sites located upstream of the *HEY1* transcription start site (+1). Primer sequences flanking the -488 to -216 bp region contained two putative NFI binding sites, at -332 to

317 bp and -411 to -396 bp, and primers flanking the -822 to -628 bp region contained one putative NFI binding site, at -794 to -779 bp. The *GAPDH* promoter was used as the negative control. Input DNA was obtained from cells lysed after the sonication step.

Electrophoretic Mobility Shift Assay (EMSA)

EMSA were carried out as previously described [39]. Putative NFI binding sequences in the *HEY1* promoter are listed in Figure 1A. Complementary oligonucleotides (Figure 2B) were annealed and radiolabeled by Klenow polymerase in the presence of $\alpha^{32}\text{P}$ -deoxycytidine triphosphate. Oligonucleotides containing mutated NFI binding sites were generated by substituting AA for the conserved GG at positions 3 and 4 of the NFI consensus binding site (Figure 2A). Nuclear extracts were prepared from untransfected U251 GBM cells as described previously [40], and nuclear extracts from U251 GBM cells transfected with pCH, pCH-NFIA, pCH-NFIB, pCH-NFIC, and pCH-NFIX were prepared using the Thermo Scientific NE-PER Nuclear and Cytoplasmic Extraction Kit (Life Technologies). Nuclear extracts (3 μg for untransfected U251 GBM cells, 2 μg for pCH-transfected cells, 3 μg for pCH-NFIA-transfected cells, 4 μg for pCH-NFIB-transfected cells, 1 μg for pCH-NFIC-transfected cells, and 2 μg for pCH-NFIX-transfected cells) were preincubated in binding buffer (20 mM Hepes pH 7.9, 20 mM KCl, 1 mM spermidine, 10 mM dithiothreitol, 10% glycerol, 0.1% Nonidet P-40) in the presence of 1.25 μg poly(dI-dC) for 10 minutes at room temperature. Where indicated, a 100× molar excess of competitor oligonucleotide was included during preincubation. Radiolabeled oligonucleotides were added to the reaction mixture and incubated for 20 minutes at room temperature.

(a)

NFI consensus binding site: TTGGC(NNNNN)GCCAA

-32 to -17 bp	5'-TTGCC(GCCCC)GCCTC-3'
-332 to -317 bp	5'-CTGGC(GCGCG)GCCAG-3'
-411 to -396 bp	5'-TTGGC(TGGCG)GCCGC-3'
-794 to -779 bp	5'-TGGGC(TGGTG)GCCAC-3'

(b)

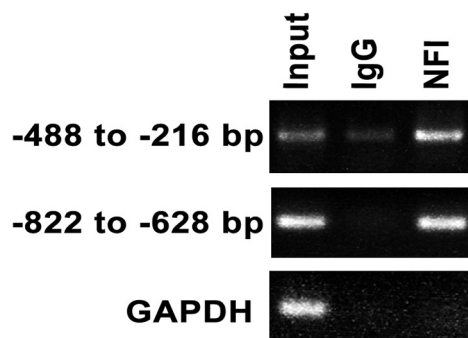


Figure 1. NFI binds to the *HEY1* promoter *in vivo*. (A) Location of consensus NFI binding sites and putative NFI binding sequences identified upstream of the *HEY1* transcription start site (+1). (B) Chromatin immunoprecipitation analysis showing NFI binding to the *HEY1* promoter. DNA cross-linked to protein in U251 cells was immunoprecipitated with a pan-specific NFI antibody followed by PCR amplification. Rabbit IgG antibody and GAPDH primers were used as negative controls.

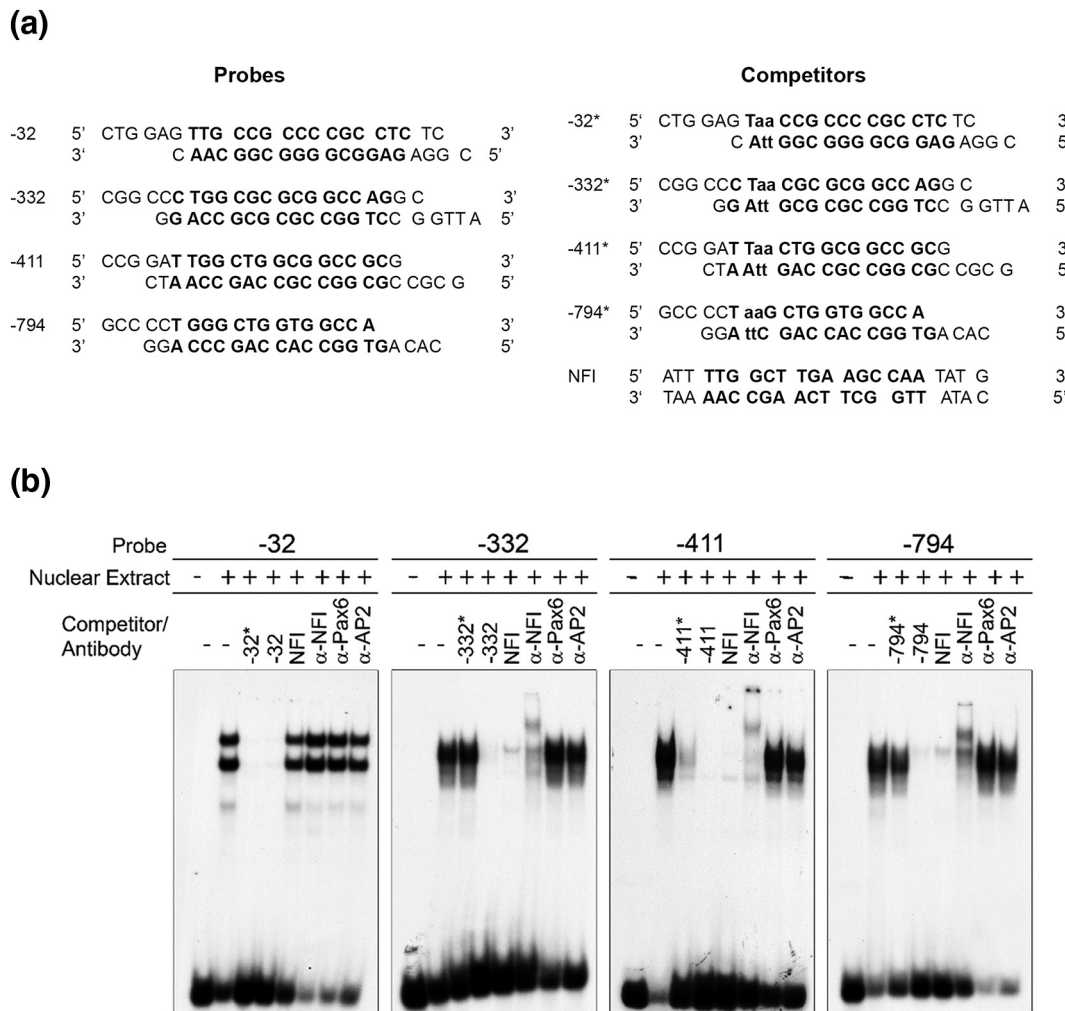


Figure 2. Binding of NFI to putative NFI binding sequences in the *HEY1* promoter. (A) Primers used to generate oligonucleotides for the electrophoretic mobility shift assay, with putative NFI binding sequences in bold. The third and fourth residues in the NFI binding sequences were mutated from GG \rightarrow AA. These residues are critical for NFI binding. (B) Electrophoretic mobility shift assays were carried out by incubating radiolabeled probes -32 bp, -332 bp, -411 bp, and -794 bp with 3 μ g U251 GBM nuclear extracts. DNA-protein complexes were electrophoresed through a 6% polyacrylamide gel buffered in 0.5 \times TBE. Where indicated, a 100 \times molar excess of competitors (* denotes mutated NFI binding site) was added to the binding reaction. Where indicated, antibodies (1 μ l) to NFI (α -NFI), Pax6 (α -Pax6), or AP2 (α -AP2) were added immediately before the radiolabeled probes.

For supershift experiments, 1 μ l anti-NFI antibody (a gift from Dr. N. Tanese, New York University Medical Center), 1 μ l anti-AP2 antibody (negative control) (Santa Cruz Biotechnology), or 1 μ l anti-Pax6 (negative control) (Developmental Studies Hybridoma Bank) was added with the radiolabeled oligonucleotides. DNA-protein complexes were electrophoresed in 6% native polyacrylamide gels in 0.5 \times TBE buffer and exposed to film.

Western Blot Analysis

Nuclear extracts were prepared using Thermo-Scientific NE-PER Nuclear and Cytoplasmic Extraction Kit (Life Technologies). Nuclear extracts were electrophoresed through 8% polyacrylamide-SDS gels and transferred to polyvinylidene fluoride (PVDF) membranes. Membranes were immunostained with mouse anti-HA antibody (Sigma) (1:10,000), rabbit anti-DDX1 antibody (1:5000) [41], or rabbit anti-HEY1 antibody (ARP32512, Aviva Systems Biology) (1:200). Primary antibodies were detected with horseradish peroxidase-conjugated secondary antibodies (Jackson ImmunoResearch Biotech) using Immobilon (EMD Millipore).

Quantitative Real Time-PCR (qPCR)

Total RNA was isolated from GBM cells using the RNeasy Plus Kit (Qiagen), and cDNA was synthesized with Superscript II reverse transcriptase (Life Technologies). qPCR was carried out using an ABI 7900HT Fast Real-Time PCR System, with gene-specific oligonucleotides labeled at the 5' end with the fluorescent reporter dye FAM (NFIA, Hs00325656_m1; NFIB, Hs00232149_m1; NFIC, Hs00907819_m1; NFIX, Hs00958849_m1; GFAP, Hs00157674_m1; B-FABP, Hs00361426_m1; NES, Hs04187831_g1; HEY1, Hs01114113_m1; GAPDH, Hs99999905_m1) and Taqman Fast Master Mix (Life Technologies). All samples were assayed in triplicate, and gene expression was normalized to *GAPDH*. Experiments were repeated three times.

Reporter Gene Assay

U251 GBM cells were cultured in 12-well cell culture plates. Following transfection, cells were harvested in 250 μ l of 1 \times Luciferase Cell Culture Lysis Buffer (Promega) and stored at -80 $^{\circ}$ C. Luciferase activity was measured in 20- μ l aliquots of lysate following addition of 100 μ l of Luciferase Assay Reagent (Promega) using a FLUOstar Optima microplate reader (BMG Labtech).

Cell Proliferation Assay

U251 GBM cells cultured under standard conditions (DMEM supplemented with 10% FCS) and A4-004 GBM cells cultured under neurosphere conditions were transfected with scrambled or HEY1 siRNAs. Forty-eight hours later, transfected cells were seeded in triplicate (30,000 cells per well) in a 12-well plate. Cell growth was measured by counting the cells in triplicate wells every 24 hours for a period of 96 hours using a Coulter Particle and Size Analyzer (Coulter Corporation). Data from three independent experiments were averaged and plotted on a graph.

Scratch assay

U251 and A4-004 cells were cultured and transfected with either scrambled or HEY1 siRNAs as described for the cell proliferation assay. Cells were seeded in triplicate in 12-well plates 48 hours posttransfection. Cells were allowed to form a monolayer, at which time a scratch was made in the center of the wells using a P20 pipette tip. Cells were cultured for an additional 24 hours (A4-004) or 30 hours (U251). Digital imaging microscopy (Axiovert 200M, Zeiss) was used to image the cells at two separate positions in each well using a phase contrast lens at 10 \times magnification (six positions in total for triplicate wells). Metamorph imaging software (Version 7.8.8.0, Molecular Devices) was used to capture a total of 97 images at each position at 15-minute intervals over a period of 24 or 30 hours. TScratch software was used to analyze the images. The percentage open area of the scratch at different time points was measured. The open area of each scratch at 0 hour was normalized to 100% to nullify the effects of minor differences in the initial scratch size in different wells. The open area at subsequent time points is represented relative to their respective 0-hour time point. Three independent experiments were carried out for each cell line.

Transwell Migration Assay

U251 and A4-004 cells were cultured and transfected with either scrambled or HEY1 siRNAs as described for the cell proliferation assay. Directional cell migration was measured using the Transwell cell migration assay. Twenty-five thousand cells in DMEM containing 1% fetal calf serum were seeded in the top chambers of 24-well cell culture Transwell inserts (Falcon Cell Culture Inserts). Cells were allowed to migrate through an 8- μ m polyethylene terephthalate (PET) membrane towards a chemoattractant (DMEM +10% fetal calf serum) in the bottom chamber for 20 hours. Cells were then fixed with 100% cold methanol for 20 minutes and stained with 1% crystal violet in 20% methanol for 30 minutes at room temperature. Migrated cells were imaged using a Zeiss Axioskop2 plus microscope by capturing different fields of view. Cell counting was carried out using Meta express imaging software. Three independent experiments were carried out for each cell line tested.

Neurosphere Formation Assay

Either 200 or 1000 cells were seeded in triplicate in a 24-well low attachment plate (Corning). Cells were allowed to form spheres for a period of 10 days. Digital imaging microscopy (Axiovert 200M, Zeiss) was used to image the spheres using a phase contrast lens at 10 \times magnification. Total area of all the spheres in each well was calculated for each treatment using Meta express imaging software. Experiments were repeated three times.

Statistical Analysis

ChIP-on-chip results from two microarray sets were analyzed using ChIP Analytics software (Agilent Technologies). Identification of putative NFI targets was based on the following parameters: enriched binding to NFI (compared to IgG control) based on a cutoff of Log (2) ratio >0.85 (enrichment of 1.8 \times) ($P < .01$). All other experiments were done in triplicate (technical replicated) and were repeated three times (biological replicates). The data shown in the graphs represent an average of all three independent experiments. The statistical significance between two treatments was calculated using an unpaired t test.

Results

ChIP-on-chip of NFI Binding Regions in GBM Cells

To identify NFI target genes in GBM cells, U251 cells were treated with 1% formaldehyde to cross-link DNA to proteins. Cell lysates were prepared and sonicated to shear the DNA into fragments of ~500 bp. A pan-specific NFI antibody was used to pull down NFIs bound to DNA. This NFI-bound DNA was hybridized to two Agilent Human Promoter 1 arrays (Agilent Technologies) containing probes from -5.5 kb upstream to +2.5 kb downstream from the transcription start site of ~17,000 RefSeq genes. The data were analyzed with ChIP Analytics software (Agilent Technologies), resulting in the identification of 403 genes with enriched NFI binding based on a cutoff of log (2) ratio >0.85 (enrichment of >1.8-fold) ($P < .01$) (Supplementary Table S1). The list includes previously identified NFI target genes including *GFAP* [36,42,43], *CDKN1A* (p21) [29,44], and *NEFL* (neurofilament light) [13].

Gene ontology (GO) enrichment analysis (GO biological process complete annotation data set, 27,378 terms) of NFI putative target genes revealed enrichment in several developmental processes, including system development, organ morphogenesis, differentiation, and specifically cardiovascular, skeletal, and neuronal development (Supplementary Table S2) [45,46]. NFI target genes were also enriched in the category of genes involved in regulation of gene expression, both positive and negative, and transcription from RNA pol II promoters (Supplementary Table S2), suggesting that NFI itself may regulate other transcription factors. In addition, GO enrichment

Table 1. PANTHER Enrichment Analysis of Putative NFI Target Genes Identified by ChIP-on-chip

GO Term	Sample Frequency	Expected Frequency	Fold Enrichment	P Value
Developmental process	85	49.6	1.71	9.02E-05
Cellular process	144	103.73	1.39	9.56E-04
Regulation of biological process	65	37.91	1.71	2.75E-03
System development	51	28.67	1.78	1.07E-02
Biological regulation	84	56.68	1.48	2.55E-02
Nervous system development	34	17.57	1.94	4.70E-02

GO analysis of putative NFI target genes was carried out. The GO terms represent the biological processes involved.

analysis using the PANTHER GO-slim Biological Process annotation data set, which contains 257 biological process terms, clearly highlights enrichment in development, specifically nervous system development (Table 1) [47].

Binding of NFI to the *HEY1* Promoter

Of the 403 putative NFI binding regions identified by ChIP-on-chip, 221 were in the promoter regions of genes. One of the putative NFI target genes, *HEY1*, was of particular interest because of its role as a Notch effector gene [48]. *HEY1* has previously been shown to be important for maintenance of neural precursor cells [34] and is highly expressed in GBM tumors compared to normal brain [35].

ChIP analysis showed enriched binding of NFI to a microchip probe corresponding to the region upstream of the *HEY1* transcription start site. Sequence analysis of the *HEY1* promoter region from -1100 bp to +1 revealed four putative NFI binding sites located at -32 to -17 bp, -332 to -317 bp, -411 to -396 bp, and -794 to -779 bp (Figure 1A). Of note, the region spanning -30 to -247 bp upstream of the mouse *Hey1* transcription start site has previously been reported to be essential for basal *Hey1* transcription, with additional regulatory sequences located between

-247 and -647 bp in mouse (with -647 bp corresponding to -680 bp in human) [49].

To confirm the ChIP-on-chip results, we carried out ChIP analysis in U251 GBM cells using primers corresponding to two regions of the *HEY1* promoter: -216 to -488 bp containing two putative NFI binding sites and -628 to -822 bp containing one putative NFI binding site. DNA cross-linked to NFI in U251 cells was immunoprecipitated with a pan-specific NFI antibody and amplified by PCR. Rabbit IgG and primers to the *GAPDH* promoter were used as negative controls for the ChIP experiments. Bands corresponding to the *HEY1* promoter between -488 to -216 bp and -822 to -628 bp were clearly detected and enriched following immunoprecipitation with an NFI antibody compared to rabbit IgG (Figure 1B). No bands were detected in either the IgG or NFI IP lanes when primers to the *GAPDH* promoter were used.

Binding of NFI to NFI Recognition Sequences in the *HEY1* Promoter

We used the EMSA to examine NFI binding to the four putative NFI recognition sites (at -32 bp, -332 bp, -411 bp, and -794 bp) located upstream of the *HEY* gene. Double-stranded oligonucleotides

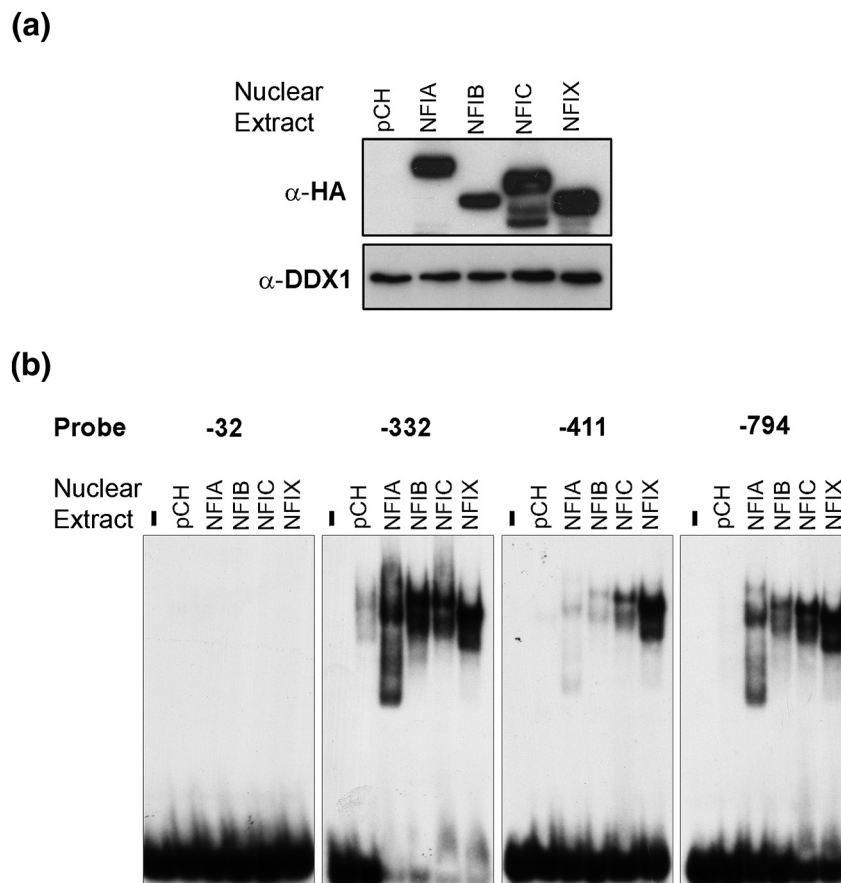


Figure 3. Binding of NFIA, NFIB, NFIC, and NFIX to NFI binding sites in the *HEY1* promoter. Nuclear extracts were prepared from U251 GBM cells transfected with control (pCH), NFIA (pCH-NFIA), NFIB (pCH-NFIB), NFIC (pCH-NFIC), or NFIX (pCH-NFIX) expression constructs. (A) Western blot analysis of transfected cells. Nuclear extracts (20 μ g) were electrophoresed through an 8% polyacrylamide-SDS gel, electroblotted onto PVDF membranes, and immunostained with α -HA antibody or α -DDX1 antibody. (B) Electrophoretic mobility shift assays were performed with the indicated radiolabeled probes: -32 bp, -332 bp, -411 bp, and -794 bp. Probes were incubated with the indicated nuclear extracts (2 μ g pCH, 3 μ g NFIA, 4 μ g NFIB, 1 μ g NFIC, and 2 μ g NFIX). Amounts of protein were adjusted to compensate for differences in expression of transfected HA-NFIs. DNA-protein complexes were electrophoresed through a 6% polyacrylamide gel buffered in 0.5 \times TBE.

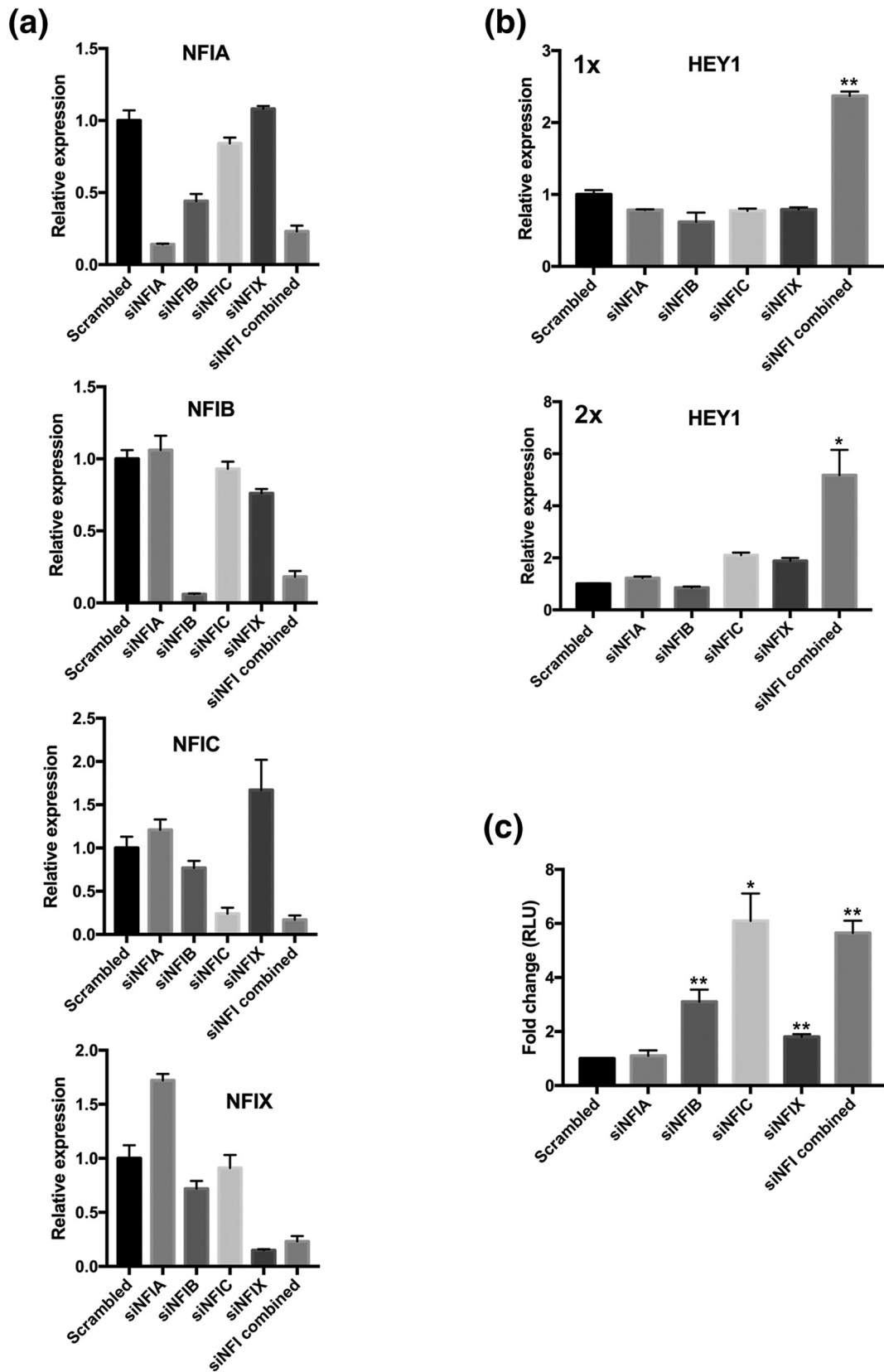
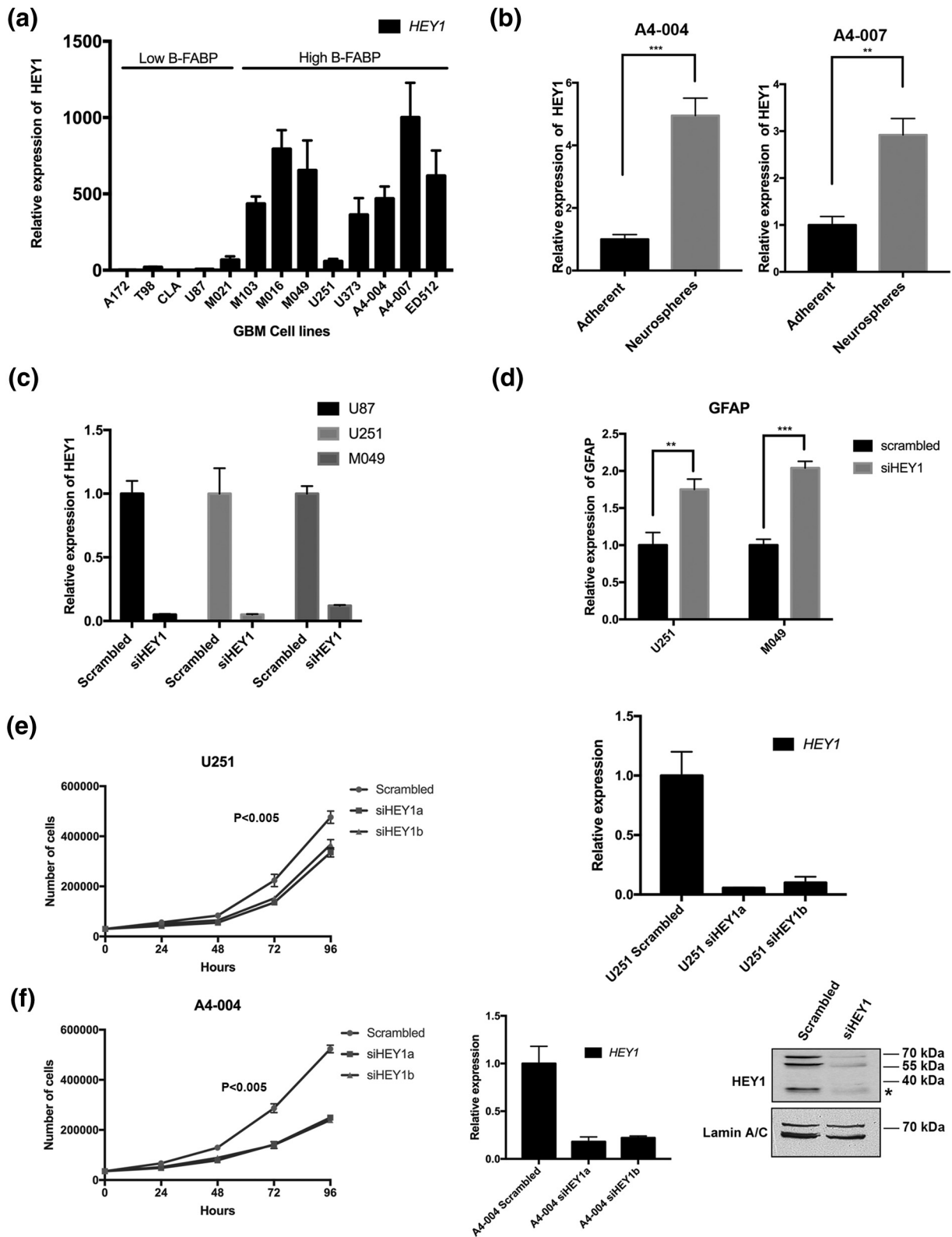


Figure 4. Regulation of *HEY1* promoter activity by NFI. U251 GBM cells were transfected with 10 nM siRNAs, including control (scrambled), NFIA, NFIB, NFIC, NFIX, or combinations of NFI siRNAs. Where indicated (2×), cells underwent two rounds of siRNA transfection. (A) *NFIA*, *NFIB*, *NFIC*, *NFIX*, and (B) *HEY1* mRNA expression was analyzed by qPCR. GAPDH was used as an endogenous control. Similar data were obtained in two separate experiments. (C) U251 GBM cells were transfected with 10 nM siRNAs, including control (scrambled), NFIA, NFIB, NFIC, NFIX, or combinations of NFI siRNAs, followed 24 hours later by transfection with pGL3/*HEY1*. Cells were harvested 60 hours later, and luciferase activity was quantified. Changes in relative light units (RLU) are relative to RLU obtained in U251 GBM cells transfected with control (scrambled) siRNA and pGL3/*HEY1*. The data are from three experiments. SEM is indicated by error bars. Statistical significance, determined using the unpaired *t* test, is indicated by * ($P < .05$) and ** ($P < .01$).



(Figure 2A) corresponding to each putative recognition site were radiolabeled and incubated with nuclear extracts prepared from U251 GBM cells. To address specificity of binding, a 100×-fold molar excess of unlabeled oligonucleotides was used as a competitor. Competitor oligonucleotides included wild-type -32 bp, -332 bp, -411 bp, -794 bp, and mutated -32* bp, -332* bp, -411* bp, -794* bp NFI recognition sites, and the NFI consensus recognition site (Figure 2A).

Two strong and one weak DNA-protein complexes were observed when the -32 bp probe was incubated with nuclear extracts from U251 GBM cells, and one major DNA-protein complex was observed upon incubation of these nuclear extracts with the -332 bp, -411 bp, and -794 bp probes (Figure 2B). Incubation with excess mutated -32* bp oligonucleotide (two key NFI binding residues mutated) resulted in complete loss of shifted bands, indicating that the DNA-protein

complexes observed with the -32 bp probe do not involve NFI binding. These data are further supported by the inability of excess NFI consensus binding site oligonucleotide to serve as competitor for the three DNA-protein complexes observed with the -32 bp probe.

In contrast to the -32 bp probe, addition of excess wild-type competitor oligonucleotides abolished binding to the -332 bp, -411 bp, and -794 bp probes, while addition of excess NFI consensus oligonucleotide significantly reduced the signal intensity of the DNA-protein complexes (Figure 2B). Addition of excess -332* bp oligonucleotide did not significantly affect binding to the radiolabeled -332 bp probe, whereas addition of excess -411* bp and -794* bp oligonucleotides resulted in significant and slight reductions in binding, respectively.

To determine if the observed DNA-protein complexes contain NFI, we incubated the radiolabeled probes with nuclear extracts from U251 GBM cells and an anti-NFI antibody that has previously been shown to supershift NFI-DNA complexes [7,36]. Addition of the anti-NFI antibody resulted in a supershifted band for the -332 bp, -411 bp, and -794 bp probes but not the -32 bp probe (Figure 2B). The relatively weak intensity of the supershifted bands observed with the anti-NFI antibody, combined with the significant decrease in intensity of the DNA-protein complexes, suggests that the anti-NFI antibody impedes binding of NFI to these probes. Alternatively, the weak supershift could be due to the relatively low levels of NFI in U251 cells [7], with the shifted band consisting primarily of non-NFI proteins. Anti-Pax6 and anti-AP2 antibodies had no effect on the protein-DNA complexes regardless of the probe used.

As there are four NFIs, we next asked whether specific members of the NFI family can preferentially bind to the NFI recognition motifs upstream of the *HEY1* transcription start site. To do this experiment, U251 GBM cells were transfected with pCH (empty vector), HA-tagged NFIA, HA-NFIB, HA-NFIC, or HA-NFIX expression constructs. Nuclear extracts were prepared, and expression of NFIs was analyzed by Western blot. NFIC levels were the highest in the transfected cells, followed by NFIX, NFIA, and NFIB (Figure 3A). To correct for differences in expression levels, we incubated 1 μ g of NFIC nuclear extract, 2 μ g NFIX nuclear extract, 3 μ g NFIA nuclear extract, and 4 μ g of NFIB nuclear extract with radiolabeled -32 bp, -332 bp, -411 bp, and -794 bp oligonucleotides. As expected, no DNA-protein complexes were observed with the -32 bp oligonucleotide, indicating that NFIs do not bind to this region.

NFIA, NFIB, NFIC, and NFIX all formed complexes with the -332 bp, -411 bp, and -794 bp oligonucleotides (Figure 3B). Bands of similar intensities were observed when nuclear extracts prepared from each of the four HA-NFI transfected cells were incubated with the -332 bp probe.

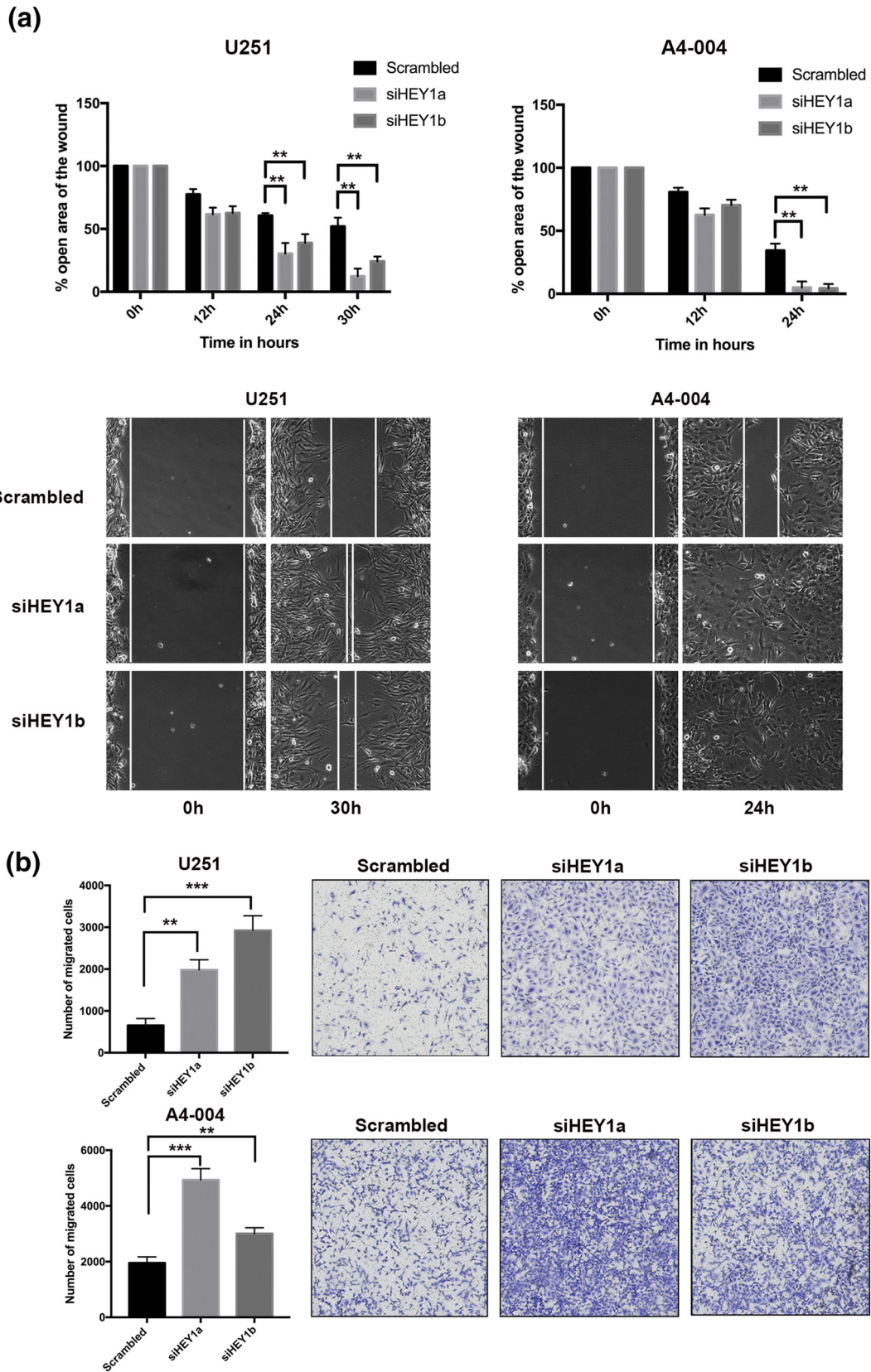
Similar results were obtained with the -794 bp probe except that band intensities were reduced in the NFIA and NFIB lanes compared to NFIC and NFIX (Figure 3B). In contrast, the only nuclear extract that generated a strong signal when incubated with the -411 bp probe was from HA-NFIX-transfected cells, with only weak bands observed with HA-NFIA and HA-NFIB-transfected cells. Taken together, these results indicate that all four NFIs can bind, albeit with different affinities, to the -332 bp, -411 bp, and -794 bp probes, with NFIA and NFIB showing a relative preference for the -332 bp probe, NFIX showing no preference for any of the three probes, and NFIC showing preference for the -332 bp and -794 bp probes.

Repression of *HEY1* Expression and Promoter Activity by NFI

Our combined ChIP and gel shift experiments indicate that NFIs bind to three distinct regions in the *HEY1* promoter, suggesting a role for NFIs in the regulation of *HEY1* expression. We therefore examined whether changes in NFI levels can affect endogenous *HEY1* mRNA levels. U251 GBM cells were transfected with control (scrambled) siRNAs, or siRNAs targeting specific NFIs, alone or in combination. Previously validated NFI siRNAs [36] were used for these analyses, resulting in 75%-93% decreases in *NFIA*, *NFIB*, *NFIC*, and *NFIX* mRNA levels after one round of transfection (Figure 4A). Endogenous levels of *HEY1* mRNA were not significantly altered upon knockdown of single NFIs; however, when all four NFIs were depleted, we observed a 2.4-fold increase in *HEY1* mRNA levels (Figure 4B, top panel). Two rounds of NFI siRNA transfections resulted in an even greater increase (4.6-fold) in *HEY1* mRNA levels (Figure 4B, bottom panel). These data suggest that multiple members of the NFI family are involved in *HEY1* regulation, with NFIs repressing *HEY1* promoter activity.

Next, we used the luciferase reporter gene under the control of the *HEY1* promoter to investigate the effect of NFI on transcriptional activity. U251 GBM cells were transfected with siRNAs to knock down single NFIs or a combination of all four NFIs, followed by transfection with the pGL3/*HEY1* construct containing -915 to +15 bp of the *HEY1* promoter upstream of the firefly luciferase reporter gene. Knockdown of NFIA did not affect *HEY1* transcriptional activity based on the luciferase assay (Figure 4C). However, transcriptional activity was significantly increased following knockdown of NFIB (3.1-fold), NFIC (6.1-fold), and NFIX (1.6-fold), suggesting that these three NFIs repress transcription from the *HEY1* promoter. Knockdown of all four NFIs increased transcriptional activity 5.6-fold compared to control (scrambled) siRNA. As the biggest increase in *HEY1* transcriptional activity was observed upon NFIC knockdown, with a similar effect seen upon knockdown

Figure 5. *HEY1* expression and effect of *HEY1* knockdown on *GFAP* RNA levels and cell proliferation. (A) qPCR analysis showing *HEY1* mRNA levels in a panel of standard (adherent) and patient-derived GBM cell lines. The first five cell lines have no or low B-FABP expression, and the rest of the cell lines express high levels of B-FABP. (B) qPCR analysis showing *HEY1* mRNA levels in A4-004 and A4-007 GBM cells cultured under standard (adherent) or neurosphere culture conditions. (C, D) U87, U251, and M049 GBM cells were transfected with 10 nM control (scrambled) siRNA or siRNA targeting *HEY1* and harvested 60 hours later. Relative *HEY1* (C) and *GFAP* (D) mRNA levels were measured by qPCR. GAPDH served as an endogenous control. RNA levels are expressed as fold-change normalized to scrambled control. (E, F) U251 GBM and A4-004 (neurosphere) cells were transfected with either scrambled siRNA or siRNAs targeting *HEY1* (siHE1a or siHE1b). Cell proliferation was measured by counting cells every 24 hours for a period of 96 hours using a Coulter counter. Thirty thousand cells per well were seeded in triplicate. qRT-PCR was used to measure the efficiency of *HEY1* knockdown. Experiments were repeated three times for each cell line. The unpaired *t* test was used to measure statistical significance. A Western blot showing reduced levels of *HEY1* upon *HEY1* knockdown in A4-004 cells is also shown in (F). The asterisk points to the band of the predicted *HEY1* size (33 kDa). Higher-molecular weight bands may represent posttranslationally modified *HEY1* proteins. ** represents $P < .01$; *** represents $P < .001$.



of all four NFIs, these results suggest that NFIC is a key player in the repression of *HEY1* promoter activity, at least in the context of an extrachromosomal plasmid reporter gene assay. The combinatorial effect of NFIs on endogenous *HEY1* mRNA levels (Figure 4B) clearly indicates that multiple members of the NFI family are involved in endogenous *HEY1* regulation.

HEY1 Expression in GBM Cells

HEY1 expression has previously been reported in the developing central nervous system and in GBM tumors [34,35]. We carried out quantitative PCR analysis to measure relative *HEY1* mRNA levels in a panel of standard GBM cell lines (adherent; cultured in medium containing fetal calf serum), as well as GBM patient-derived adherent

cell lines (cultured in medium containing fetal calf serum) and tumor neurosphere cultures (serum-free; medium supplemented with growth factors) (Figure 5, A and B). Overall, there was a trend towards lower *HEY1* RNA levels in cell lines that expressed low levels of the neural stem cell marker B-FABP [50–53] (Figure 5A). High *HEY1* RNA levels were observed in all three GBM tumor neurosphere cell lines tested (A4-004, A4-007, and ED512) (Figure 5A). When we compared adherent cultures and tumor neurosphere cultures derived from the same patient, we observed considerably higher levels of *HEY1* RNA in the neurosphere cultures, in keeping with *HEY1* being more highly expressed in tumor cells with neural stem cell properties (Figure 5B).

In the developing brain, *HEY1* is required for the maintenance of neural precursor cells [34], whereas *NFIA* is required for initiation of gliogenesis and astrocyte differentiation [14,18]. To address a possible role for *HEY1* in the prevention of astrocyte differentiation, we transfected *HEY1* siRNAs into three GBM cell lines: U87 (very low levels of *HEY1*; does not express astrocyte differentiation marker *GFAP*), U251 (low levels of *HEY1*; expresses *GFAP*), and M049 (high levels of *HEY1*; expresses *GFAP*). *HEY1* RNA levels were decreased by 85% to 94% in cells transfected with *HEY1* siRNA compared to control (scrambled) siRNA (Figure 5C). *HEY1* knockdown had no effect on *GFAP* RNA levels in U87 cells, indicating that *HEY1* depletion is not sufficient to induce *GFAP* expression in cells that do not express endogenous *GFAP*. However, there was a ~2× increase in *GFAP* RNA levels in U251 (1.8-fold) and M049 (2-fold) GBM cells upon *HEY1* depletion (Figure 5D). While these results do not address the biological relevance of a 2× increase in *GFAP* RNA levels, they are in keeping with a role for *HEY1* in the maintenance of neural stem cell properties.

Effects of *HEY1* Depletion on Cell Proliferation and Migration in GBM

We transfected U251 GBM cells and A4-004 neurosphere cultures with *HEY1* siRNAs to examine the effect of *HEY1* knockdown on cell proliferation and migration. Both *HEY1* siRNAs used for these experiments decreased *HEY1* RNA levels by >90% (U251) and ~80% (A4-004) (Figure 5, E and F). *HEY1* protein levels were also reduced by >70% upon *HEY1* depletion (Figure 5F). *HEY1* knockdown in both these cell lines resulted in decreased cell proliferation compared to cells transfected with control siRNAs (Figure 5, E and F).

Next, we measured the cell motility of U251 and A4-004 cells transfected with either control or *HEY1* siRNAs using the scratch assay. *HEY1*-depleted U251 and A4-004 cells both showed increased motility compared to control cells, closing the wound (scratch) significantly faster than cells transfected with control siRNAs (Figure 6A; see Supplementary Figure S1 for 95% confidence intervals). In U251 cells, depletion of *HEY1* by two different siRNAs (siHE1Y1a and siHE1Y1b) resulted in

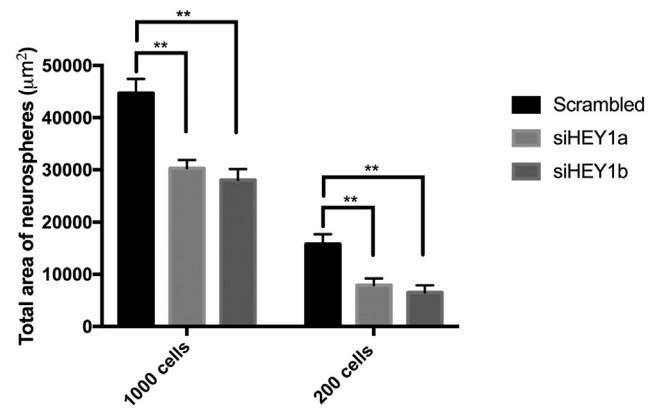


Figure 7. *HEY1* knockdown reduces neurosphere formation. Either 200 or 1000 A4-004 cells were seeded in triplicate in a 24-well low-attachment plate. Cells were allowed to form spheres for a period of 10 days. Sphere formation was analyzed by measuring the total area of all the spheres in each well. The results are from three independent experiments. The unpaired *t* test was used to measure statistical significance. ** represents $P < .01$.

~4.3-fold and ~2.2-fold increases in cell motility, respectively. In A4-004, *HEY1* depletion resulted in 7- to 8-fold increases in cell motility. We also used the Transwell migration assay to measure the migration of *HEY1*-depleted cells compared to control cells. In keeping with the results obtained with the scratch assay, *HEY1*-depleted U251 and A4-004 GBM cells showed significantly higher migration rates compared to cells transfected with control siRNAs. Specifically, U251 cells transfected with two different siRNAs showed approximately 3.70- and 5.37-fold increases in migration compared to control transfectants (Figure 6B; see Supplementary Figure S1 for 95% confidence intervals). *HEY1*-depleted A4-004 cells showed 2.57- and 1.53-fold increases in migration compared to cells transfected with scrambled (control) siRNAs.

HEY1 Depletion and Neurosphere Formation

We transfected A4-004 cells with *HEY1* siRNAs to examine the effect of *HEY1* knockdown on their ability to form neurospheres. Either 1000 or 200 cells were seeded in triplicate in low-attachment 24-well plates and were allowed to form spheres over a period of 10 days. *HEY1* depletion resulted in decreased numbers of neurospheres as well as smaller neurospheres. We therefore measured the total area of all the neurospheres in each well. When 1000 cells were seeded, there was a decrease of 32% and 37% in total neurosphere area in siHEY1a and siHEY1b transfected cells, respectively. When 200 cells were seeded, the decrease in total area was 50% and 59% for the two *HEY1* siRNAs compared to control siRNAs (Figure 7; see Supplementary Figure S1 for 95% confidence intervals).

Figure 6. *HEY1* knockdown results in reduced cell migration. (A) U251 GBM and A4-004 (neurosphere) cells were transfected with either scrambled siRNAs or siRNAs against *HEY1* (siHEY1a or siHEY1b) and allowed to reach confluency. A scratch was made in the center of each well, and cells were allowed to migrate over a period of 30 hours (U251) or 24 hours (A4-004) with live cell monitoring. Graphs represent percentage open area of the wound (scratch). Each experiment was carried out in triplicate with data obtained from six different positions for each time point. Experiments were repeated three times, and the unpaired *t* test was used to measure statistical significance. Images shown represent 0 hour and 30 hours (U251) or 24 hours (A4-004) time points. (B) Transwell cell migration assay showing reduced cell migration upon *HEY1* knockdown. Twenty-five thousand cells were seeded in the upper chamber and allowed to migrate across a PET membrane towards medium containing 10% FCS over a period of 24 hours. Migrated cells were fixed, stained, and counted using Metamorph imaging software. The data shown in the graphs represent an average of three independent experiments. The unpaired *t* test was used to measure statistical significance. ** represents $P < .01$; *** represents $P < .001$.

Discussion

The NFI family is an important regulator of glial cell differentiation during development [14], with a well-characterized role in the regulation of glial differentiation genes, including *GFAP*, in both normal brain and GBM cells [36]. We used a ChIP-on-chip approach to identify additional NFI target genes in GBM. DNA sequences from a total of 403 genes were found to be preferentially bound by NFI using a pan-specific anti-NFI antibody. GO analysis of putative NFI target genes identified enrichment of genes involved in multiple biological processes including gene expression, development, and differentiation and, of particular interest, genes involved in nervous system development.

One of the 403 genes identified by ChIP-on-chip was the Notch effector gene *HEY1*. The HEY family consists of three basic helix-loop-helix (bHLH) proteins (HEY1, HEY2, and HEYL) closely related to the HES family of transcriptional repressors [54]. HEY1 is normally expressed in undifferentiated cells of the developing mouse brain [34]. Ectopic expression of HEY1 in the developing mouse brain inhibits neurogenesis and promotes maintenance of undifferentiated cells [34]. Promoter assays indicate that HEY1 acts by inhibiting the neuronal bHLH genes *Ascl1* (also known as *Mash1*) and *Neurod4* (also known as *Math3*) [34].

We identified four putative NFI binding sites within a 1000-bp region immediately upstream of the *HEY1* transcription start site. Gel shift assays revealed NFI binding to three of these four putative sites: at -794 bp, -411 bp, and -332 bp. Although multiple protein-DNA complexes were obtained with the putative NFI binding site at -32 bp, these complexes were competed out with excess cold oligonucleotide mutated at critical NFI binding residues and were not supershifted using anti-NFI antibody, indicating that proteins other than NFI bind to the -32 bp region. Combined data from gel shift and supershift experiments indicate that NFIs bind to the other three NFI recognition sites, at -332 bp, -411 bp, and -794 bp. Gel shift experiments using nuclear extracts prepared from cells that ectopically express individual NFIs indicate differential NFI binding to these three sites, with the -411 bp site being the most discriminatory, as only NFIX binds effectively to this region.

Differential binding by different NFI family members *in vitro* has been previously reported [55,56]. For example, the differential DNA binding specificities of NFI-A4, NFI-B2 and NFI-X1 for the CoRE response element located upstream of the *WAP* gene were shown to be dependent on other transcription factors binding to this region [56]. As all four NFIs have highly similar DNA binding domains and bind DNA as either homodimers or heterodimers, binding site specificity may be due to NFI interacting partners, structural changes within NFI transcription factors caused by alternative splicing or posttranslational modifications, as well as the relative levels of the different members of the NFI family [55,57]. Thus, differences in the sequences of the three NFI binding sites upstream of the *HEY1* gene may allow preferred binding to subsets of NFI recognition sites. In this regard, it is interesting to note that the main differences between the -411 bp NFI recognition sites and that of -332 bp and -794 bp are the last two nucleotides (GC in the case of -411 bp and AG and AC in the case of the -332 and -794 bp regions, respectively) (Figure 1A).

A requirement for knockdown of all four NFIs to detect an effect on endogenous *HEY1* RNA levels suggests complex regulation and cross talk between NFI family members. There is considerable variability in the transactivation domain of NFI family members [10,12], and the transactivation potential of heterodimers has

previously been reported to be intermediate to that of NFI homodimers [11]. Thus, knockdown of single NFIs, with accompanying changes in NFI interactions, may alter the dynamics of NFI dimerization in the cell but may still result in little to no effect on endogenous *HEY1* mRNA levels in the context of an intact cell. It is only when all four NFIs are depleted that their repressive effect on the *HEY1* promoter can be overcome. In contrast to the endogenous promoter, single knockdown of NFIB, NFIC, or NFIX, but not NFIA, was sufficient to induce exogenous *HEY1* promoter activity. Differences in regulation of NFI-dependent promoter activity in an endogenous (or chromosomal) context compared to an ectopic (or extrachromosomal) context have previously been reported for a number of promoters including *B-FABP*, *GFAP*, and *MMTV* [36,58]. This difference has been explained by a looser organization of the nucleosome structure in episomal DNA compared to chromosomal DNA, allowing easier access to transcription factors [59].

HEY1 expression in GBM correlates with increased tumor grade and decreased survival [60]. Similar to the results reported here, others have shown that HEY1 knockdown decreases proliferation in U87, T98, and U373 GBM cell lines as well as GBM lines established from mouse xenografts [35,61]. We extend these studies by demonstrating that HEY1 is associated with higher levels of the neural stem cell marker B-FABP in GBM cells and increased neurosphere formation, in keeping with its proposed role in the brain [34]. Furthermore, HEY1 depletion in GBM cells that already express the astrocyte differentiation marker GFAP results in increased *GFAP* mRNA levels. In contrast to a previous report indicating that HEY1 knockdown resulted in decreased migration in GBM cell lines [61], our results indicate a significant increase in migration upon HEY1 depletion in GBM cells. This discrepancy may stem from the fact that the pooled siRNAs used for HEY1 depletion by Tsung et al. resulted in increased apoptosis in GBM cell lines established from mouse xenografts [61]. Thus, our results support roles for NFIs and HEY1 in controlling fundamental pro-growth versus anti-growth properties of GBM, as well as support the “go or grow” hypothesis whereby cells with reduced proliferation show increased migration and *vice versa* [33].

In contrast to HEY1, high *NFIA* and *NFIB* mRNA levels correlate with improved patient survival in astrocytomas, with reduced expression of NFIA and NFIB associated with higher-grade astrocytomas [28,30]. In the developing CNS, NFIA and NFIB drive the onset of gliogenesis (gliogenic switch) [14,15,18,19], with NFIX playing a role in the later stages of astrocyte differentiation [20,62]. *Nfia*^{-/-}, *Nfib*^{-/-}, and *Nfix*^{-/-} null mice all show delays in the differentiation of glial cells in developing brain [21–27]. Although NFIC is widely expressed in the CNS, *Nfic* knockout in mice causes tooth pathologies rather than brain defects, suggesting that its roles in brain are redundant with other NFIs [22,63]. Several studies have shown that NFIs, especially NFIA and NFIB, positively regulate the expression of genes associated with glial cell differentiation (e.g., *GFAP*, *SPARCL1*, *APCDD1*, *MMD2*) [18,42,43,62] while repressing genes associated with stem cell maintenance (*EZH2*, *HES1*) [17,64]. As previously reported, the association between reduced levels of NFIA/NFIB and increased malignancy in astrocytoma is in agreement with NFIs playing similar roles in gliogenesis and gliomagenesis; i.e., promotion of glial cell differentiation properties [65,66]. Our results indicating that NFI knockdown upregulates *HEY1* expression add to the repertoire of genes controlled by NFIs that determine stemness versus differentiation properties. It is a well-

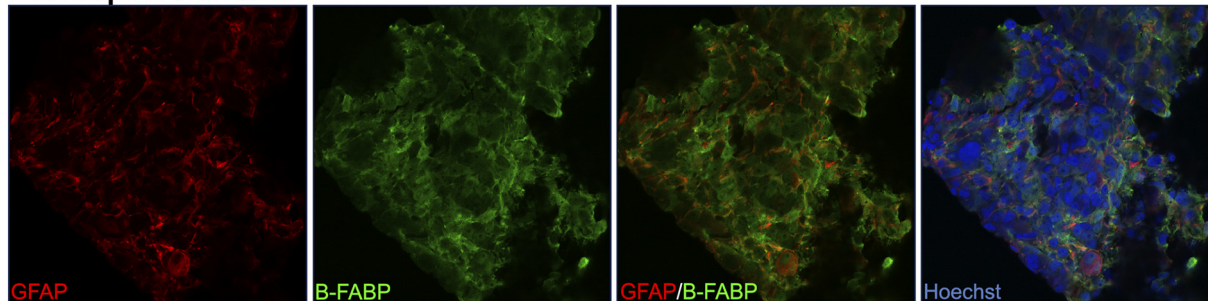
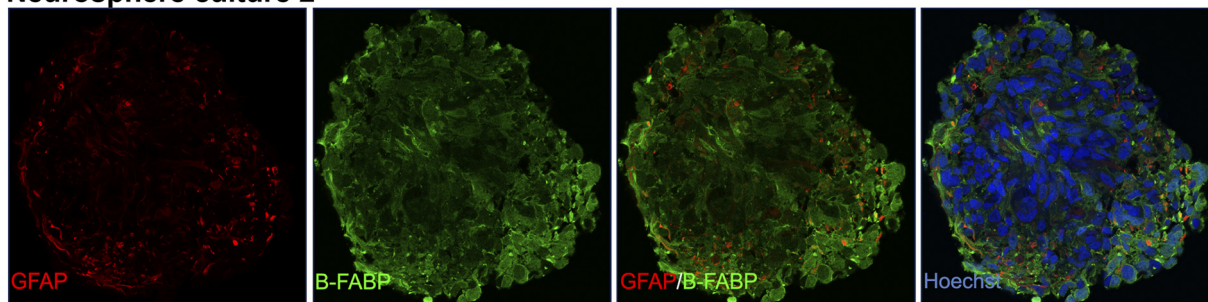
Neurosphere culture 1**Neurosphere culture 2**

Figure 8. Immunofluorescence analysis of GBM neurospheres. Neurospheres from two patient-derived GBM neurosphere cultures were fixed in formalin and embedded in paraffin. Sections were immunostained with anti-GFAP and anti-B-FABP antibodies. The signal was detected with secondary antibodies conjugated to Alexa 555 (red; GFAP) or Alexa 488 (green; B-FABP). Hoechst 33342 was used to label the nuclei. Heterogeneity in B-FABP and GFAP expression was observed in both neurosphere cultures.

known fact that there is considerable heterogeneity in GBM tumors and the cell lines derived from these tumors. Thus, within a single tumor or cell line, there may be NFI-high cells associated with expression of astrocytic markers and less aggressive growth properties, and NFI-low cells associated with increased stemness and more aggressive growth properties. In support of this idea, examination of the astrocytic marker GFAP and neural stem/progenitor cell marker B-FABP in GBM neurosphere cultures reveals little overlap in the expression of these two markers (Figure 8).

Conclusions

In summary, we show that NFI transcription factors expressed in GBM cells bind to the promoters of multiple genes involved in many biological processes. We identify three NFI binding sites in the *HEY1* promoter and show that NFI represses *HEY1* promoter activity and expression in GBM cells. We demonstrate differential binding of the four members of the NFI family to the different NFI binding sites in the *HEY1* promoter. Our results indicate complex interactions between the different members of the NFI family and suggest that NFI dimerization, along with additional transcription factors, is involved in the regulation of the *HEY1* gene in GBM. The decrease in cell proliferation and neurosphere formation, along with the increase in cell migration observed upon *HEY1* knockdown, supports the “go or grow” hypothesis previously validated for a number of tumor models. We propose that mutually exclusive cell migration and proliferation in GBM cells can be explained at least in part by relative levels of NFIs and *HEY1*.

Acknowledgements

We are grateful to Dr. Richard Gronostajski for his gift of the pCHNFI expression constructs and to Dr. Naoko Tanese for the

anti-NFI antibody used for the supershift experiments. We thank Dr. Xuejun Sun, Gerry Barron, and the Cross Cancer Institute Cell Imaging Facility for their support with imaging cells and neurospheres. This work was supported by Canadian Institutes of Health Research grant number 130314.

Appendix A. Supplementary data

Supplementary data to this article can be found online at <https://doi.org/10.1016/j.neo.2018.08.007>.

References

- [1] Ohgaki H and Kleihues P (2005). Population-based studies on incidence, survival rates, and genetic alterations in astrocytic and oligodendroglial gliomas. *J Neuropathol Exp Neurol* **64**, 479–489.
- [2] Dolecek TA, Propp JM, Stroup NE, and Kruchko C (2012). CBTRUS statistical report: primary brain and central nervous system tumors diagnosed in the United States in 2005–2009. *Neuro Oncol* **14**(Suppl. 5), v1–49.
- [3] Stupp R, Mason WP, van den Bent MJ, Weller M, Fisher B, Taphoorn MJ, Belanger K, Brandes AA, Marosi C, and Bogdahn U, et al (2005). Radiotherapy plus concomitant and adjuvant temozolomide for glioblastoma. *N Engl J Med* **352**, 987–996.
- [4] Mason WP, Maestro RD, Eisenstat D, Forsyth P, Fulton D, Laperriere N, Macdonald D, Perry J, and Thiessen B (2007). Canadian recommendations for the treatment of glioblastoma multiforme. *Curr Oncol* **14**, 110–117.
- [5] Cloughesy TF, Cavenee WK, and Mischel PS (2014). Glioblastoma: from molecular pathology to targeted treatment. *Annu Rev Pathol* **9**, 1–25.
- [6] Wang H, Xu T, Jiang Y, Xu H, Yan Y, Fu D, and Chen J (2015). The challenges and the promise of molecular targeted therapy in malignant gliomas. *Neoplasia* **17**, 239–255.
- [7] Bisgrove DA, Monckton EA, Packer M, and Godbout R (2000). Regulation of brain fatty acid-binding protein expression by differential phosphorylation of nuclear factor I in malignant glioma cell lines. *J Biol Chem* **275**, 30668–30676.
- [8] Gronostajski RM (1986). Analysis of nuclear factor I binding to DNA using degenerate oligonucleotides. *Nucleic Acids Res* **14**, 9117–9132.
- [9] Kruse U, Qian F, and Sippel AE (1991). Identification of a fourth nuclear factor I gene in chicken by cDNA cloning: NFI-X. *Nucleic Acids Res* **19**, 6641.

- [10] Kruse U and Sippel AE (1994). Transcription factor nuclear factor I proteins form stable homo- and heterodimers. *FEBS Lett* **348**, 46–50.
- [11] Chaudhry AZ, Vitullo AD, and Gronostajski RM (1998). Nuclear factor I (NFI) isoforms differentially activate simple versus complex NFI-responsive promoters. *J Biol Chem* **273**, 18538–18546.
- [12] Gronostajski RM (2000). Roles of the NFI/CTF gene family in transcription and development. *Gene* **249**, 31–45.
- [13] Amemiya K, Traub R, Durham L, and Major EO (1992). Adjacent nuclear factor-I and activator protein binding sites in the enhancer of the neurotropic JC virus. A common characteristic of many brain-specific genes. *J Biol Chem* **267**, 14204–14211.
- [14] Deneen B, Ho R, Lukaszewicz A, Hochstim CJ, Gronostajski RM, and Anderson DJ (2006). The transcription factor NFIA controls the onset of gliogenesis in the developing spinal cord. *Neuron* **52**, 953–968.
- [15] Namihira M, Kohyama J, Semi K, Sanosaka T, Deneen B, Taga T, and Nakashima K (2009). Committed neuronal precursors confer astrocytic potential on residual neural precursor cells. *Dev Cell* **16**, 245–255.
- [16] Mason S, Piper M, Gronostajski RM, and Richards LJ (2009). Nuclear factor one transcription factors in CNS development. *Mol Neurobiol* **39**, 10–23.
- [17] Piper M, Barry G, Hawkins J, Mason S, Lindwall C, Little E, Sarkar A, Smith AG, Moldrich RX, and Boyle GM, et al (2010). NFIA controls telencephalic progenitor cell differentiation through repression of the Notch effector Hes1. *J Neurosci* **30**, 9127–9139.
- [18] Kang P, Lee HK, Glasgow SM, Finley M, Donti T, Gaber ZB, Graham BH, Foster AE, Novitsch BG, and Gronostajski RM, et al (2012). Sox9 and NFIA coordinate a transcriptional regulatory cascade during the initiation of gliogenesis. *Neuron* **74**, 79–94.
- [19] Glasgow SM, Zhu W, Stolt CC, Huang TW, Chen F, LoTurco JJ, Neul JL, Wegner M, Mohila C, and Deneen B (2014). Mutual antagonism between Sox10 and NFIA regulates diversification of glial lineages and glioma subtypes. *Nat Neurosci* **17**, 1322–1329.
- [20] Matuzelski E, Bunt J, Harkins D, Lim JWC, Gronostajski RM, Richards LJ, Harris L, and Piper M (2017). Transcriptional regulation of Nfix by NFIB drives astrocytic maturation within the developing spinal cord. *Dev Biol* **432**, 286–297.
- [21] das Neves L, Duchala CS, Tolentino-Silva F, Haxhiu MA, Colmenares C, Macklin WB, Campbell CE, Butz KG, and Gronostajski RM (1999). Disruption of the murine nuclear factor I-A gene (Nfia) results in perinatal lethality, hydrocephalus, and agenesis of the corpus callosum. *Proc Natl Acad Sci USA* **96**, 11946–11951.
- [22] Steele-Perkins G, Plachez C, Butz KG, Yang G, Bachurski CJ, Kinsman SL, Litwack ED, Richards LJ, and Gronostajski RM (2005). The transcription factor gene Nfib is essential for both lung maturation and brain development. *Mol Cell Biol* **25**, 685–698.
- [23] Driller K, Pagenstecher A, Uhl M, Omran H, Berlis A, Grunder A, and Sippel AE (2007). Nuclear factor I X deficiency causes brain malformation and severe skeletal defects. *Mol Cell Biol* **27**, 3855–3867.
- [24] Heng YH, McLeay RC, Harvey TJ, Smith AG, Barry G, Cato K, Plachez C, Little E, Mason S, and Dixon C, et al (2014). NFIX regulates neural progenitor cell differentiation during hippocampal morphogenesis. *Cereb Cortex* **24**, 261–279.
- [25] Betancourt J, Katzman S, and Chen B (2014). Nuclear factor one B regulates neural stem cell differentiation and axonal projection of corticofugal neurons. *J Comp Neurol* **522**, 6–35.
- [26] Shu T, Butz KG, Plachez C, Gronostajski RM, and Richards LJ (2003). Abnormal development of forebrain midline glia and commissural projections in Nfia knock-out mice. *J Neurosci* **23**, 203–212.
- [27] Wong YW, Schulze C, Streichert T, Gronostajski RM, Schachner M, and Tilling T (2007). Gene expression analysis of nuclear factor I-A deficient mice indicates delayed brain maturation. *Genome Biol* **8**, R72.
- [28] Song HR, Gonzalez-Gomez I, Suh GS, Commins DL, Sposto R, Gilles FH, Deneen B, and Erdreich-Epstein A (2010). Nuclear factor IA is expressed in astrocytomas and is associated with improved survival. *Neuro Oncol* **12**, 122–132.
- [29] Lee JS, Xiao J, Patel P, Schade J, Wang J, Deneen B, Erdreich-Epstein A, and Song HR (2014). A novel tumor-promoting role for nuclear factor IA in glioblastomas is mediated through negative regulation of p53, p21, and PAI1. *Neuro Oncol* **16**, 191–203.
- [30] Stringer BW, Bunt J, Day BW, Barry G, Jamieson PR, Ensby KS, Bruce ZC, Goasdoué K, Vidal H, and Charmsaz S, et al (2016). Nuclear factor one B (NFIB) encodes a subtype-specific tumour suppressor in glioblastoma. *Oncotarget* **7**, 29306–29320.
- [31] Bayin NS, Ma L, Thomas C, Baitalmal R, Sure A, Fansiwala K, Bustoros M, Golfinos JG, Pacione D, and Snuderl M, et al (2016). Patient-specific screening using high-grade glioma explants to determine potential radiosensitization by a TGF-beta small molecule inhibitor. *Neoplasia* **18**, 795–805.
- [32] Lino MM, Merlo A, and Boulay JL (2010). Notch signaling in glioblastoma: a developmental drug target? *BMC Med* **8**, 72.
- [33] Mehta S and Lo Cascio C (2018). Developmentally regulated signaling pathways in glioma invasion. *Cell Mol Life Sci* **75**, 385–402.
- [34] Sakamoto M, Hirata H, Ohtsuka T, Bessho Y, and Kageyama R (2003). The basic helix-loop-helix genes Hes1/Hes2 and Hes2/Hes2 regulate maintenance of neural precursor cells in the brain. *J Biol Chem* **278**, 44808–44815.
- [35] Hulleman E, Quarto M, Vernell R, Masserdotti G, Colli E, Kros JM, Levi D, Gaetani P, Tunici P, and Finocchiaro G, et al (2009). A role for the transcription factor HEY1 in glioblastoma. *J Cell Mol Med* **13**, 136–146.
- [36] Brun M, Coles JE, Monckton EA, Glubrecht DD, Bisgrove D, and Godbout R (2009). Nuclear factor I regulates brain fatty acid-binding protein and glial fibrillary acidic protein gene expression in malignant glioma cell lines. *J Mol Biol* **391**, 282–300.
- [37] Godbout R, Bisgrove DA, Shkolny D, and Day III RS (1998). Correlation of B-FABP and GFAP expression in malignant glioma. *Oncogene* **16**, 1955–1962.
- [38] Pillai S, Dasgupta P, and Chellappan SP (2009). Chromatin immunoprecipitation assays: analyzing transcription factor binding and histone modifications in vivo. *Methods Mol Biol* **523**, 323–339.
- [39] O'Brien RM, Noisin EL, Suwanichkul A, Yamasaki T, Lucas PC, Wang JC, Powell DR, and Granner DK (1995). Hepatic nuclear factor 3- and hormone-regulated expression of the phosphoenolpyruvate carboxykinase and insulin-like growth factor-binding protein 1 genes. *Mol Cell Biol* **15**, 1747–1758.
- [40] Roy RJ, Gosselin P, and Guerin SL (1991). A short protocol for micro-purification of nuclear proteins from whole animal tissue. *Biotechniques* **11**, 770–777.
- [41] Bleoo S, Sun X, Hendzel MJ, Rowe JM, Packer M, and Godbout R (2001). Association of human DEAD box protein DDX1 with a cleavage stimulation factor involved in 3'-end processing of pre-mRNA. *Mol Biol Cell* **12**, 3046–3059.
- [42] Cebolla B and Vallejo M (2006). Nuclear factor-I regulates glial fibrillary acidic protein gene expression in astrocytes differentiated from cortical precursor cells. *J Neurochem* **97**, 1057–1070.
- [43] Gopalan SM, Wilczynska KM, Konik BS, Bryan L, and Kordula T (2006). Nuclear factor-1-X regulates astrocyte-specific expression of the alpha1-antichymotrypsin and glial fibrillary acidic protein genes. *J Biol Chem* **281**, 13126–13133.
- [44] Ouellet S, Vigneault F, Lessard M, Leclerc S, Drouin R, and Guerin SL (2006). Transcriptional regulation of the cyclin-dependent kinase inhibitor 1A (p21) gene by NFI in proliferating human cells. *Nucleic Acids Res* **34**, 6472–6487.
- [45] Ashburner M, Ball CA, Blake JA, Borstein D, Butler H, Cherry JM, Davis AP, Dolinski K, Dwight SS, and Eppig JT, et al (2000). Gene ontology: tool for the unification of biology. The Gene Ontology Consortium. *Nat Genet* **25**, 25–29.
- [46] *Gene Ontology Consortium: going forward* *Nucleic Acids Res* **43**, D1049–D1056.
- [47] Mi H, Muruganujan A, and Thomas PD (2013). PANTHER in 2013: modeling the evolution of gene function, and other gene attributes, in the context of phylogenetic trees. *Nucleic Acids Res* **41**, D377–D386.
- [48] Iso T, Kedes L, and Hamamori Y (2003). HES and HERP families: multiple effectors of the Notch signaling pathway. *J Cell Physiol* **194**, 237–255.
- [49] Maier MM and Gessler M (2000). Comparative analysis of the human and mouse Hey1 promoter: Hey genes are new Notch target genes. *Biochem Biophys Res Commun* **275**, 652–660.
- [50] Mita R, Coles JE, Glubrecht DD, Sung R, Sun X, and Godbout R (2007). B-FABP-expressing radial glial cells: the malignant glioma cell of origin? *Neoplasia* **9**, 734–744.
- [51] Morihito Y, Yasumoto Y, Vaidyan LK, Sadahiro H, Uchida T, Inamura A, Sharifi K, Ideguchi M, Nomura S, and Tokuda N, et al (2013). Fatty acid binding protein 7 as a marker of glioma stem cells. *Pathol Int* **63**, 546–553.
- [52] Rosa A, Pellegatta S, Rossi M, Tunici P, Magnoni L, Speranza MC, Malusa F, Miragliotta V, Mori E, and Finocchiaro G, et al (2012). A radial glia gene marker, fatty acid binding protein 7 (FABP7), is involved in proliferation and invasion of glioblastoma cells. *PLoS One* **7**, e52113.
- [53] Yasumoto Y, Miyazaki H, Vaidyan LK, Kagawa Y, Ebrahimi M, Yamamoto Y, Yamada T, Katagiri H, and Owada Y (2016). Inhibition of fatty acid synthase

- decreases expression of stemness markers in glioma stem cells. *PLoS One* **11**e0147717.
- [54] Nakagawa O, Nakagawa M, Richardson JA, Olson EN, and Srivastava D (1999). HRT1, HRT2, and HRT3: a new subclass of bHLH transcription factors marking specific cardiac, somitic, and pharyngeal arch segments. *Dev Biol* **216**, 72–84.
- [55] Osada S, Matsubara T, Daimon S, Terazu Y, Xu M, Nishihara T, and Imagawa M (1999). Expression, DNA-binding specificity and transcriptional regulation of nuclear factor 1 family proteins from rat. *Biochem J* **342**(Pt 1), 189–198.
- [56] Mukhopadhyay SS, Wyszomierski SL, Gronostajski RM, and Rosen JM (2001). Differential interactions of specific nuclear factor I isoforms with the glucocorticoid receptor and STAT5 in the cooperative regulation of WAP gene transcription. *Mol Cell Biol* **21**, 6859–6869.
- [57] Liu Y, Bernard HU, and Apt D (1997). NFI-B3, a novel transcriptional repressor of the nuclear factor I family, is generated by alternative RNA processing. *J Biol Chem* **272**, 10739–10745.
- [58] Archer TK, Lefebvre P, Wolford RG, and Hager GL (1992). Transcription factor loading on the MMTV promoter: a bimodal mechanism for promoter activation. *Science* **255**, 1573–1576.
- [59] Hebbar PB and Archer TK (2008). Altered histone H1 stoichiometry and an absence of nucleosome positioning on transfected DNA. *J Biol Chem* **283**, 4595–4601.
- [60] Gaetani P, Hulleman E, Levi D, Quarto M, Scorsetti M, Helins K, and Simonelli M (2010). Expression of the transcription factor HEY1 in glioblastoma: a preliminary clinical study. *Tumori* **96**, 97–102.
- [61] Tsung AJ, Guda MR, Asuthkar S, Labak CM, Purvis IJ, Lu Y, Jain N, Bach SE, Prasad DVR, and Velpula KK (2017). Methylation regulates HEY1 expression in glioblastoma. *Oncotarget* **8**, 44398–44409.
- [62] Wilczynska KM, Singh SK, Adams B, Bryan L, Rao RR, Valerie K, Wright S, Griswold-Prenner I, and Kordula T (2009). Nuclear factor I isoforms regulate gene expression during the differentiation of human neural progenitors to astrocytes. *Stem Cells* **27**, 1173–1181.
- [63] Lee TY, Lee DS, Kim HM, Ko JS, Gronostajski RM, Cho MI, Son HH, and Park JC (2009). Disruption of Nfic causes dissociation of odontoblasts by interfering with the formation of intercellular junctions and aberrant odontoblast differentiation. *J Histochem Cytochem* **57**, 469–476.
- [64] Piper M, Barry G, Harvey TJ, McLeay R, Smith AG, Harris L, Mason S, Stringer BW, Day BW, and Wray NR, et al (2014). NFIB-mediated repression of the epigenetic factor Ezh2 regulates cortical development. *J Neurosci* **34**, 2921–2930.
- [65] Chen KS, Lim JWC, Richards LJ, and Bunt J (2017). The convergent roles of the nuclear factor I transcription factors in development and cancer. *Cancer Lett* **410**, 124–138.
- [66] Chen KS, Harris L, Lim JWC, Harvey TJ, Piper M, Gronostajski RM, Richards LJ, and Bunt J (2017). Differential neuronal and glial expression of nuclear factor I proteins in the cerebral cortex of adult mice. *J Comp Neurol* **525**, 2465–2483.